Switchable magnetic moment in cobalt-doped graphene bilayer on Cu(111): An *ab initio* study

Everson S. Souza*
Departamento de Física, Universidade Federal do Espírito Santo, Vitória, ES, Brazil

Wanderlã L. Scopel†
Departamento de Física, Universidade Federal do Espírito Santo, Vitória, ES, Brazil
and Departamento de Ciências Exatas, Universidade Federal Fluminense, Volta Redonda, RJ, Brazil

R. H. Miwa‡
Instituto de Física, Universidade Federal de Uberlândia, Uberlândia, MG, Brazil
(Received 19 October 2015; revised manuscript received 20 April 2016; published 20 June 2016)

In this work, we have performed an *ab initio* theoretical investigation of substitutional cobalt atoms in the graphene bilayer supported on the Cu(111) surface (Co/GBL/Cu). Initially, we examined the separated systems, namely, graphene bilayer adsorbed on Cu(111) (GBL/Cu) and a free standing Co-doped GBL (Co/GBL). In the former system, the GBL becomes *n*-type doped, where we map the net electronic charge density distribution along the GBL–Cu(111) interface. The substitutional Co atom in Co/GBL lies between the graphene layers, and present a net magnetic moment mostly due to the unpaired Co-3d_{z^2} electrons. In Co/GBL/Cu, we found that the Cu(111) substrate rules (i) the energetic stability, and (ii) the magnetic properties of substitutional Co atoms in the graphene bilayer. In (i), the substitutional Co atom becomes energetically more stable lying on the GBL surface, and in (ii), the magnetic moment of Co/GBL has been quenched due to the Cu(111) → Co/GBL electronic charge transfer. We verify that such a charge transfer can be tuned upon the application of an external electric field, and thus mediated by a suitable change on the electronic occupation of the Co-d_{z^2} orbitals, we found a way to switch-on and -off the magnetization of the Co-doped GBL adsorbed on the Cu(111) surface.

DOI: 10.1103/PhysRevB.93.235308

I. INTRODUCTION

The experimental isolation of graphene monolayer [1] and bilayer [2] has aroused great interest in the fundamental research of two-dimensional (2D) layered materials [3]. In parallel, the functionalization of those 2D crystals has been the subject of several studies; where the substitutional doping has been a promising route to adjust/tune their electronic and magnetic properties.

Recent experimental studies demonstrate the possibility of inserting substitutional Co atoms in graphene monolayer upon the presence of vacancy defects [4]. Further theoretical studies have shown that cobalt atoms are energetically stable in single vacancy regions, with the emergence of a magnetic moment associated with the substitutional defect [4–6]. The magnetic properties of cobalt atoms in graphene may depend on the choice of the substrate on which the graphene layer is grown/supported. Such a dependence is dictated by the strength of the electronic coupling between the functionalized graphene sheet and the substrate [7].

In the last few years, pristine graphene monolayers [8–12] and bilayers [13] adsorbed on metal surfaces have been the subject of systematic theoretical studies, including different approaches to describe the van der Waals (vdW) interactions. These studies indicated that the vdW interactions play an important role in the adsorption of graphene on metal surfaces such as Al(111), Au(111), Pt(111), and Cu(111), and it becomes *n*- or *p*-type doped depending on the metal substrate. From the experimental viewpoint, the synthesis of graphene monolayer [14–17] and bilayer [18–21] on copper substrate have been successfully performed. Copper surfaces have been used as a substrate not only for pristine graphene, but also in functionalized graphene layers; like graphene monolayer doped with substitutional (nitrogen, sulfur, and boron) impurities [22–24], and asymmetrically N-doped graphene bilayer [25].

Concomitantly, the control of magnetic properties of defective graphene through electric field or doping effect is desirable for spintronics applications [26]. In this sense, experimental results have indicated a reduction of magnetization in graphene with vacancy or sp^3 impurities due to doping effect [27,28], and the possibility of controlling such a magnetic property through external electric field has been proposed. Experimental studies also indicate that doping effect, determined by the metal substrate, can affect the magnetic moment associated with defects in graphenic systems [29].

In this work, we have performed an *ab initio* theoretical investigation of substitutional cobalt atoms in graphene bilayer (Co/GBL) supported on the Cu(111) surface (Co/GBL/Cu). Our results indicate that the metal substrate plays an important role on the energetic stability, and the magnetic properties of the Co-doped graphene bilayer. Particularly, the net magnetic moment verified in free standing Co/GBL is quenched, due to the Cu(111) → Co/GBL charge transfer. We show that such a charge transfer can be mediated by an external electric field, and thus turning-on and -off the magnetization of the Co-doped GBL. Our study provides further support to the development

*nosreveazuos@gmail.com
†wlscopel@gmail.com
‡hiroki@infis.ufu.br

of magnetic switch in functionalized 2D materials adsorbed on metallic surfaces.

II. METHODOLOGY

In this work, all the calculations were performed using spin-polarized density functional theory (DFT) [30,31], as implemented in the QUANTUM ESPRESSO [32] package. We used the generalized gradient approximation (GGA) with the Perdew-Burke-Ernzerhof parametrization (GGA-PBE) [33] for exchange-correlation functional, ultrasoft potentials [34] generated with the Rappe-Rabe-Kaxiras-Joannopoulos approach [35] to describe the electron-ion interaction, and a semiempirical approach following the Grimme formula (DFT-D2 method) [36] to describe the van der Waals dispersion interactions. The plane-wave expansion was limited by the cutoff energy of 625 eV. The Brillouin zone sampling was made using the Monkhorst-Pack method [37] with a $3 \times 3 \times 1$ k points mesh and a Gaussian smearing of 0.1 eV. All calculations were made using a convergence criterion of $\approx$ 0.1 meV for total energies. The lattice parameter of graphene (optimized value 2.46 Å) was matched to Cu(111) surface (optimized value 2.56 Å). In our calculations we have used a (5×5) surface supercell, with 50 C atoms per graphene layer, and a vacuum region of 15 Å between successive periodic images along to z direction. The slab model is composed by two graphene monolayers, and four atomic layers of copper. The two lower copper layers were kept fixed, while all the other atomic layers are allowed to relax, within the accuracy that the residual force acting on each atom is smaller than 0.025 eV/Å.

We used the Resta and Kunc method [38] for study the effect of an external electric field. In this method, a saw-tooth-like potential simulating an electric field is added to the bare ionic potential. All illustrative figures of atomic structure and volumetric electron density were generated using VESTA [39].

III. RESULTS AND DISCUSSIONS

A. Graphene bilayer on Cu(111) surface, and free standing cobalt-doped graphene bilayer

Initially, we have examined the energetic stability, structural, and electronic properties of defect-free graphene bilayer on the Cu(111) surface (GBL/Cu). Following the Bernal staking for the GBL, we have considered three plausible GBL/Cu adsorption geometries, α_{top}-β_{hcp}, α_{hcp}-β_{fcc}, and α_{hcp}-β_{top}, depicted in Figs. 1(a)–1(c), respectively. The energetic stability of those GBL/Cu systems was examined by calculation of the GBL adsorption energy (E^{ads}) defined as

$$E^{ads} = E[\text{GBL}] + E[\text{Cu}] - E[\text{GBL/Cu}],$$

where E[GBL] and E[Cu] are the total energies of the isolated components, graphene bilayer and Cu(111) surface, respectively; E[GBL/Cu] is the total energy of the final GBL/Cu structure. In accordance with the present definition of the adsorption energy, $E^{ads} > 0$, represent an exothermic process.

We obtained $E^{ads} = 39.2$ meV/Å^2 [111.3 meV/(interface C atom)] for the energetically more stable α_{top}-β_{hcp} configuration [Fig. 1(a)]; followed by the α_{hcp}-β_{fcc} configuration, which is energetically less stable by 0.7 meV/Å^2 [2.0 meV/(interface C atom)] [40]. In α_{top}-β_{hcp}, the carbon atoms of the sublattice α (β) are aligned with the cooper atoms of the first (second) layer of Cu(111). At the equilibrium geometry, we found a vertical distance between the metal and the interfacial graphene layer ($d_{G\text{-}Cu}$) of 2.898 Å, and an equilibrium distance between graphene sheets ($d_{G\text{-}G}$) of 3.211 Å. The other geometry, α_{hcp}-β_{top}, is less stable than α_{top}-β_{hcp} by 4.7 meV/Å^2 [13.4 meV/(interface C atom)]. Those results allow us to infer that the α_{top}-β_{hcp} configuration is the most likely one, followed by α_{hcp}-β_{fcc} and α_{hcp}-β_{top} [41]. It is worth noting that those adsorption energy differences are comparable with that obtained for an isolated GBL; namely, the AB stacking is more stable by 3.9 meV/Å^2 (5.6 meV/C atom) [42,43] than the AA stacking, in agreement with the experimental verification of the former one. Our results, summarized in Table I, are in agreement with the previous theoretical studies [13,44].

In Fig. 2(a), we present the total charge density at the GBL–Cu(111) interface region, showing that there are no chemical bonds between the C atoms for the GBL and the

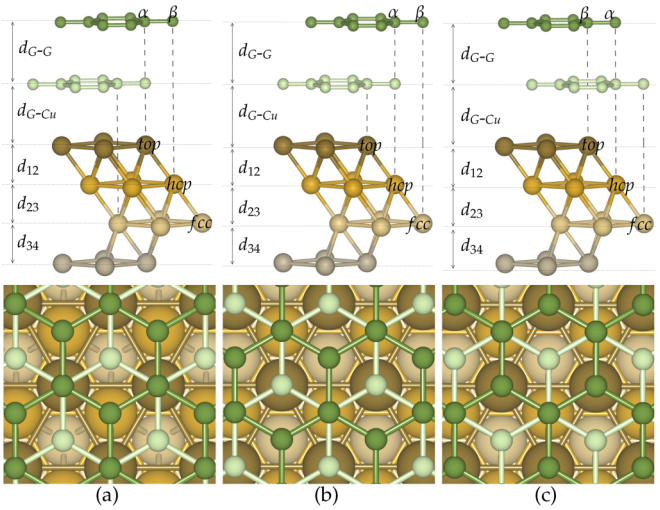

FIG. 1. Three plausible configurations for GBL/Cu interface. (a) α_{top}-β_{hcp}, (b) α_{hcp}-β_{fcc}, and (c) α_{hcp}-β_{top}. The brown, yellow, beige, and gray spheres represents cooper atoms of the first, second, third, and fourth layers of Cu(111) surface, respectively. The dark and light green spheres represent carbon atoms of the first and second graphene layers, respectively.

TABLE I. Energetic and structural properties for three different GBL/Cu adsorption geometries. Adsorption energy (E^{ads}) per area, average distance graphene-graphene ($d_{G\text{-}G}$), average distance graphene-substrate ($d_{G\text{-}Cu}$), and distances between atomic planes of Cu(111) (d_{12}, d_{23} and d_{34}). E^{ads} and distance is given in unit of meV/Å^2 and Å, respectively.

	E^{ads}	$d_{G\text{-}G}$	$d_{G\text{-}Cu}$	d_{12}	d_{23}	d_{34}
α_{top}-β_{hcp}	39.2	3.211	2.898	2.057	2.087	2.090
α_{hcp}-β_{fcc}	38.5	3.199	2.892	2.056	2.087	2.090
α_{hcp}-β_{top}	34.5	3.212	3.048	2.061	2.087	2.090

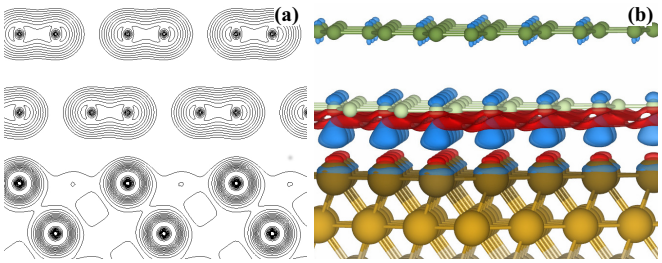

FIG. 2. (a) Total charge density at GBL–Cu(111) interface ($\rho_{GBL/Cu}$) indicating absence of overlap charge density in the region between interfacial graphene layer and copper substrate. (b) Total charge density redistribution ($\Delta\rho$) upon formation of the GBL/Cu interface. $\Delta\rho(\mathbf{r}) = \rho_{GBL/Cu}(\mathbf{r}) - \rho_{GBL}(\mathbf{r}) - \rho_{Cu}(\mathbf{r})$, where $\rho_{GBL}(\mathbf{r})$ and $\rho_{Cu}(\mathbf{r})$ represent the total charge densities of the separated systems, GBL and Cu(111) surface, both keeping the same equilibrium geometry as that of GBL/Cu, and $\rho_{GBL/Cu}(\mathbf{r})$ represents the total charge density of the final GBL/Cu system. Blue regions indicate a net charge density gain ($\Delta\rho > 0$), and red regions indicate a net charge density loss ($\Delta\rho < 0$) relative to the isolated systems. The larger and smaller spheres represent the atomic species Cu and C, respectively. Isosurface ($\pm 0.003\ e/\text{Å}^3$).

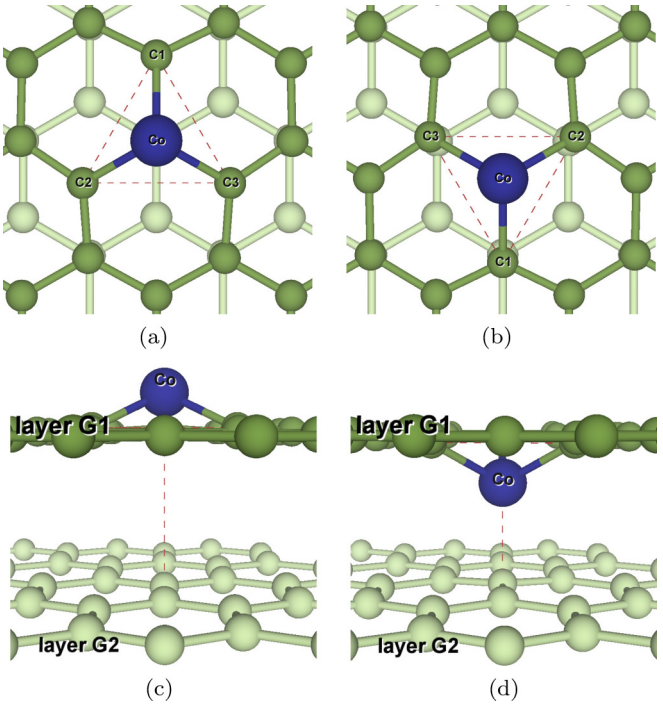

FIG. 3. Local view of the optimized atomic structures. (a) Top view of Co[α^a]/GBL, (b) top view of Co[β^a]/GBL, (c) side view of Co[α^a]/GBL, and (d) side view of Co[α^b]/GBL system. The dark and light green spheres represent carbon atoms of the first and second layer of graphene, respectively. The blue sphere represents the atomic species Co.

Cu(111) surface. However, in order to reach the electronic equilibrium, charge density redistribution will take place at the GBL–Cu(111) interface; giving rise to a net charge transfer from the Cu(111) surface to the GBL. The GBL becomes n-type doped. In Fig. 2(b), we depict the total charge density redistribution [$\Delta\rho(\mathbf{r})$] at the GBL–Cu(111) interface. We find a charge density gain at carbon atoms of the lower and upper sheets of the GBL. Based on the Bader charge density analysis, we calculate an amount of the charge transfer to the adsorbed bilayer graphene of 0.0082 e/C-atom ($5.8 \times 10^{13}\ e/\text{cm}^2$); a similar result has been obtained by using Löwdin projected orbital analysis, $6.6 \times 10^{13}\ e/\text{cm}^2$ [45]. Each layer presents a different doping level. Most of the transferred charge remains in the lower layer (83%) with a residual portion in the upper layer (17%). Such a charge density distribution gives rise to electric field between the graphene layers, removing the inversion symmetry, opening an energy gap in the GBL system [13]. The n-type doping of graphene adsorbed on Cu(111) has been experimentally observed [16,46], and supported by theoretical calculations [9,47].

Next, we examine the energetic stability and the electronic properties of an isolated (free standing) GBL doped with substitutional Co atoms (Co/GBL). We have considered Co atoms occupying carbon (single vacancy) sites of GBL. At the equilibrium geometry, since the atomic radius of cobalt atom is larger than that of carbon, the substitutional Co atom will be out of plane with respect to the graphene sheet [5]. For each nonequivalent atomic site, α/β, we find two energetically stable configurations for the substitutional Co atoms, namely, (a) Co atoms lying above of GBL surface (Co[α^a]/Co[β^a]), or (b) Co atoms between graphene sheets (Co[α^b]/Co[β^b]). For a visual understanding, in Figs. 3(a) and 3(b), we present the top-views of Co[α^a]/ and Co[β^a]/GBL, respectively, and Figs. 3(c) and 3(d) show the side-views of Co[α^a]/ and Co[α^b]/GBL, respectively.

By comparing the total energies, we find an energetic preference for Co atoms intercalated between graphene layers, Co[α^b]/ and Co[β^b]/GBL, being the former configuration more stable by 0.26 eV/Co atom; Co[α^a]/ and Co[β^a]/GBL geometries are energetically less favorable than Co[α^b]/GBL by ~0.66 eV/Co atom, respectively. In a very recent theoretical study, Tang *et al.* [48] also verified the energetic preference for substitutional Co atoms between the graphene layers, namely Co[α^b]/GBL.

The net magnetic moment (m) attributed to the dangling bonds at the carbon vacancy site, V_C, has been suppressed upon the presence of substitutional Co atoms. It is worth noting that for substitutional Co atoms in graphene monolayer, we find $m = 0.78\ \mu_B$, whereas it reduces to 0.10 and 0.25 μ_B for the energetically more stable geometries, i.e., intercalated Co atoms Co[α^b]/ and Co[β^b]/GBL. Such a reduction is due to the electronic interaction between the Co atoms and the pristine graphene layer G2 (Fig. 3), Co–G2. On the other hand, the Co[α^a]/ and Co[β^a]/GBL systems present $m = 0.78\ \mu_B$ and 0.64 μ_B, respectively; since there is no Co–G2 interaction for Co atoms lying above the GBL. Indeed, the Co-$3d_{z^2}$ of Co[α^b]/ and Co[β^b]/GBL presents an exchange splitting (E_x) of 0.03 eV and 0.08 eV, respectively, whereas Co[α^a]/ and Co[β^a]/GBL present $E_x = 0.31$ and 0.20 eV. Based upon the Bader charge density analysis [49,50], we verify an amount of charge transfer to G2 of $6 \times 10^{12} e/\text{cm}^2$ for both Co[α^b]/GBL and Co[β^b]/GBL; whereas such a charge transfer to G2 has not been verified for Co[α^a]/ and Co[β^a]/GBL.

B. Cobalt-doped graphene bilayer on Cu(111)

Here we will study the energetic stability, electronic, and magnetic properties of the substitutional cobalt atoms in the bilayer graphene adsorbed on the Cu(111) surface (Co/GBL/Cu). We have considered the energetically more stable α_{top}-β_{hcp} configuration for the GBL–Cu(111) interface, and the four Co/GBL configurations described in the previous section. For a visual understanding, in Figs. 4(a) and 4(b), we present the Co[α^a]/GBL/ and Co[β^a]/GBL/Cu structures, respectively.

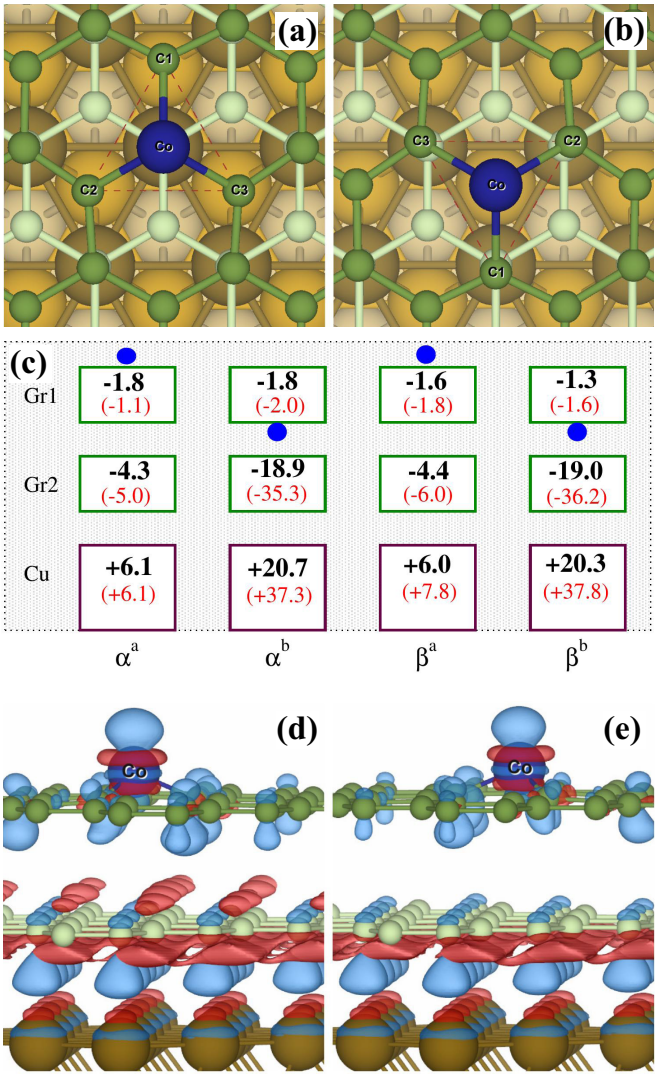

FIG. 4. Local top view of the optimized atomic structure of the (a) Co[α^a]/GBL/Cu and (b) Co[β^a]/GBL/Cu. The brown, yellow, beige, and gray spheres represents Cu atoms of the first, second, third, and fourth layers of Cu(111) surface, respectively. The dark and light green spheres represent carbon atoms of the first and second graphene layers, respectively. (c) Net total charge transfer based on the Bader (Löwdin) analysis, with respect to the isolated components, of Co/GBL/Cu in $\times 10^{13}$ e/cm^2. The blue sphere represents the (adsorbed/intercalated) atomic species Co. (d) and (e) Total charge density redistribution ($\Delta\rho$) upon formation of the Co[α^a]/GBL/Cu and Co[β^a]/GBL/Cu, respectively. Blue regions indicate a net charge density gain ($\Delta\rho > 0$), and red regions indicate a net charge density loss ($\Delta\rho < 0$) relative to the isolated components (isosurface, $\pm 0.003\ e/\text{Å}^3$).

As discussed above, the free standing Co[α^b]/ and Co[β^b]/GBL configurations are more stable than Co[α^a]/ and Co[β^a]/GBL. Upon their interaction with the Cu(111) surface, we find that the latter configurations become energetically more stable than the former ones. In order to verify the energetic stability of the Co/GBL–Cu(111) interface, we calculate the adsorption energy (E^{ads}) of the Co-doped GBL on the Cu(111) surface,

$$E^{\text{ads}} = E[\text{Co/GBL}] + E[\text{Cu(111)}] - E[\text{Co/GBL/Cu(111)}].$$

E[Co/GBL] and E[Cu(111)] represent the total energies of the separated components, Co-doped GBL and clean Cu(111) surface, respectively, and the last term, E[Co/GBL/Cu(111)], represents the total energy of the final system, Co-doped GBL adsorbed on the Cu(111) surface. The adsorption energies of Co-doped GBL, Co[α^a]/GBL/ and Co[β^a]/GBL/Cu, 39.9 and 40.1 meV/Å^2, are practically the same as that of pristine GBL on Cu(111), Table I. Whereas, for substitutional Co atoms between the graphene layers, Co[α^b]/GBL/ and Co[β^b]/GBL/Cu, the adsorption energy reduces to 35.2 and 32.7 meV/Å^2, respectively. By plotting the total charge density at the Co/GBL–Cu(111) interface (not shown), we verify that there are no chemical bonds between the (pristine) graphene sheet and the Cu(111) surface.

Here, the energetic preference for Co[α^a]/GBL/ and Co[β^a]/GBL/Cu is due to the reduction on the adsorption energy of Co[α^b]/GBL/ and Co[β^b]/GBL/Cu in comparison with the undoped system (see Table I), $E^{\text{ads}} = 39.2 \rightarrow 35.2$ and 32.7 meV/Å^2. Aiming to provide a more clear picture of such a reduction on the adsorption energy, in Fig. 4(c), we present a map of the total charge transfer at the Co/GBL–Cu(111) interface. We found that the charge transfers are larger in Co[α^b]/GBL/ and Co[β^b]/GBL/Cu; for instance, the graphene layer G2 (Cu surface) exhibits a charge density gain (reduction) of 19×10^{13} e/cm^2 (21×10^{13} e/cm^2). In contrast, for the substitutional Co atoms lying on the surface of GBL, Co[α^a]/GBL/ and Co[β^a]/GBL/Cu, such a charge density gain, and the Co/GBL–Cu(111) equilibrium distance ($d_{\text{G-Cu}} = 2.92$ Å), are close to the ones of the undoped GBL/Cu system. This latter result is in agreement with the maintenance of the adsorption energies of Co[α^a]/GBL/ and Co[β^a]/GBL/Cu in comparison with the pristine GBL/Cu system. Meanwhile, by inspection [Fig. 4(c)], we verify that the Co[α^b]/GBL/ and Co[β^b]/GBL/Cu systems present higher electrostatic energy than Co[α^a]/GBL/ and Co[β^a]/GBL/Cu, and thus reducing their adsorption energies when compared with that of GBL/Cu. Here we can infer that the electrostatic interactions, due to the electronic charge transfers in Co/GBL/Cu, rule the energetic preference of the Co[α^a]/GBL/ and Co[β^a]/GBL/Cu systems. Indeed, similar electrostatic analysis has been performed to examine the energetic stability of atomic reconstructions on semiconductor surfaces [51,52]. In Figs. 4(d) and 4(e), we present a map of the total charge transfers in Co[α^a]/ and Co[β^a]/GBL/Cu(111); where we can see that there is a net charge density gain ($\Delta\rho > 0$) (i) on the graphene layers G1 and G2, being larger in G2, and (ii) on the Co substitutional sites, Co[α^a] and Co[β^a].

Charge transfers from the Cu(111) surface to the adsorbed Co/GBL, Cu(111) → Co/GBL, promote the reduction (or suppression) of the net magnetization of the Co-doped GBL. The magnetic moments are completely quenched ($m = 0$) in Co[β^a]/GBL/, Co[β^b]/GBL/, and Co[α^b]/GBL/Cu, while it reduces to 0.35 μ_B ($m = 0.78 \rightarrow 0.35$ μ_B) in Co[α^a]/GBL/Cu. Indeed, recent studies pointed out that the electronic and magnetic properties of intrinsic defects and impurities in graphene may change upon their its interaction with metallic surfaces [29,47].

In Fig. 5, we present the PDOS of Co[α^a]/GBL/ and Co[β^a]/GBL/Cu. There is energy resonance between the Co-d_{z^2} and the C-p_z near the Fermi level. For the Co[α^a] configuration, Figs. 5(a) and 5(b), the exchange splitting of Co-d_{z^2} reduces from 0.31 eV (free standing Co[α^a]/GBL, dashed lines) to 0.14 eV (Co[α^a]/GBL/Cu, solid lines), increasing the occupation of the spin-down $3d_{z^2}$ orbital of cobalt, as well as of the nearby carbon $2p_z$ states. In contrast, such an (exchange) energy splitting is suppressed in Co[β^a]/GBL upon its interaction with the Cu(111) surface, Figs. 5(c) and 5(d). In this case, the spin-down $3d_{z^2}$ states become fully occupied, lying at around 0.3 eV below the Fermi level.

In order to improve our understanding the role of the Cu(111) surface on the quenching/suppression of the magnetic moment of Co/GBL; we simulate a n-type doping in by adding electrons to the free standing Co[α^a]/ and Co[β^a]/GBL systems. We have considered the same amount of charging as we obtained for Co[α^a]/GBL/ and Co[β^a]/GBL/Cu, 6.1×10^{13} and 5.9×10^{13} e/cm^2, respectively. We obtained $m = 0$ for both (free standing) Co/GBL systems. Those findings allow us to infer that, indeed, (i) the n-type doping rules the reduction of the magnetic moment of of Co/GBL, however, (ii) the presence of the Cu(111) surface is important, since the surface electrostatic potential will tune the charge density distribution of Co/GBL/Cu.

It is known that for weakly coupled graphene-metal interface, external electric field can be used to control the electronic and magnetic properties of graphene by controlling its doping level [27]. Indeed, very recently, Nair *et al.* [28] showed that the magnetic properties of adatoms in graphene can be tuned through the application of external electric field. Here, we apply an external electric field (EEF), perpendicularly to the Co/GBL–Cu(111) interface, aiming to control the magnetic properties of the Co/GBL adsorbed on Cu(111) [53]. EEF in the positive z direction (positive EEF) reverses the doping level, namely, there is a charge transfer (CT) from the Co/GBL to the Cu(111) surface, while EEF in the negative z direction (negative EEF) the CT occurs from the Cu(111) surface to the Co/GBL increases. Our results of Cu(111) ⇆ Co/GBL charge transfers for Co[α^a]/GBL/Cu and Co[β^a]/GBL/Cu are shown in Fig. 6(a). The Cu(111) → Co/GBL CT decreases continuously for positive EEF, and it vanishes for EEF of 0.5 V/Å, and thus suggesting that we may recover the magnetization of Co/GBL.

In Fig. 6(b), we present the magnetic moment of Co[α^a]/GBL and Co[β^a]/GBL, adsorbed on the Cu(111) surface, as a function of the EEF. It is noticeable that, although both configurations present almost the same Cu(111) ⇆ Co/GBL CT profile, the tuning of the magnetic moment of Co/GBL depends on the (local) geometry of the substitutional

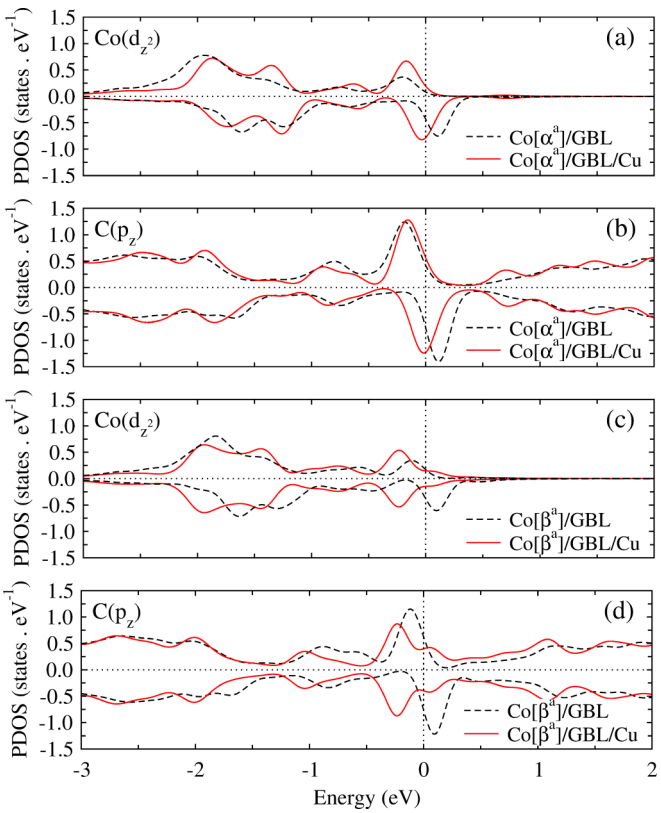

FIG. 5. Projected density of states on Co(d_{z^2}) orbital of cobalt and C(p_z) orbitals of carbon atoms in the region around of the Co defect for Co/GBL/Cu system compared with free standing Co/GBL. (a) and (b) Co[α^a] and (c) and (d) Co[β^a]. The Fermi level is set to zero.

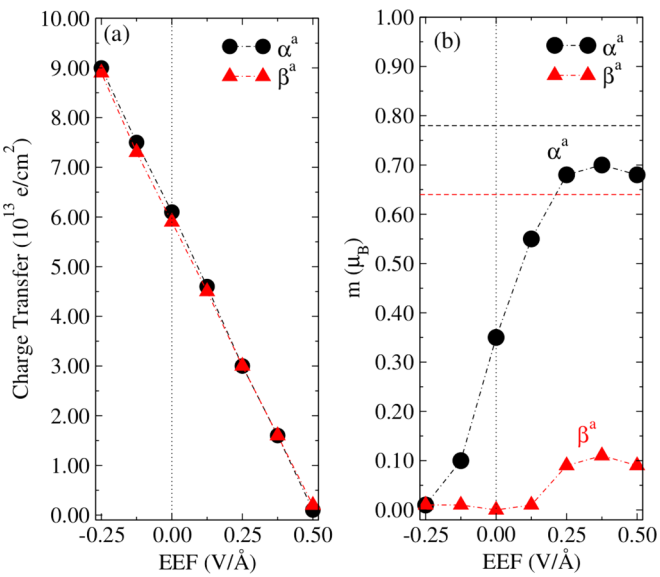

FIG. 6. (a) Cu(111) ⇆ Co/GBL charge transfers as a function of the EEF for Co[α^a]/GBL/ and Co[β^a]/GBL/Cu. (b) Magnetic moment of Co[α^a]/GBL/ and Co[β^a]/GBL/Cu as a function of the EEF. Horizontal dashed lines indicate the magnetic moment in isolated Co[α^a]/GBL (black dashed line) and Co[β^a]/GBL (red dashed line).

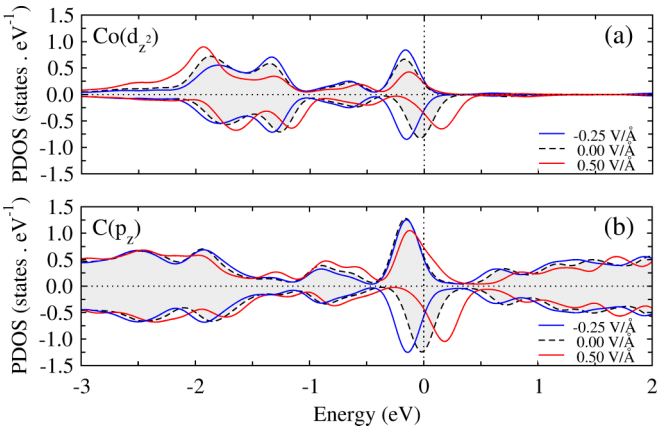

FIG. 7. Projected density of states of Co[α^a]/GBL/Cu (with an EEF of -0.25, 0 or +0.50 V/Å) on (a) the Co(d_{z^2}) orbital, (b) the C(p_z) orbitals of carbon atoms in the region around of the Co defect. The Fermi level is set to zero.

Co atom, α^a and β^a. The magnetic moment of Co[α^a]/GBL is 0.35 μ_B for EEF = 0, it is n-type doped due to its interaction with the Cu(111) surface. For positive EEF, the CT from the Co/GBL to the Cu(111) surface is followed by an increase of the magnetic moment of Co[α^a]/GBL, up to 0.70 μ_B for an EEF of +0.375 V/Å; whereas, $m \to 0$ for an EEF of -0.250 V/Å. Thus indicating that the magnetic moment of Co[α^a]/GBL/Cu can be switched on and off ($0 \leftrightarrow 0.7$ μ_B) by applying an EEF ($-0.25 \leftrightarrow +0.40$ V/Å). It is worth noting that in the free standing Co[α^a]/GBL we have $m = 0.78$ μ_B, while by tuning the EEF we obtained up to 90% of this value. Such a difference can be attributed to the change on the electronic distribution of the Co/GBL layer upon the presence of the EEF. On the other hand, the magnetic moment of Co[β^a]/GBL/Cu can be recovered only up to 16% of that of free standing configuration. As shown in Fig. 6(b), we have $m = 0.1$ μ_B for EEF of 0.375 V/Å.

The magnetization switch of Co[α^a]/GBL/Cu, controlled by the EEF, is dictated by the spin-polarization of the cobalt (α^a), and the neighboring carbon atoms. Where the changes of the (spin-up and -down) electronic population take place within an energy interval of ± 0.5 eV with respect to the Fermi level. In Fig. 7, we present the PDOS on the Co-d_{z^2}, and the neighboring C-p_z orbitals, for EEF of +0.5, 0.0, and -0.25 V/Å. For EEF of +0.5 V/Å ($m = 0.68$ μ_B), the spin-down Co-d_{z^2} orbital [Fig. 7(a)] becomes partially occupied, and present an exchange splitting of 0.28 eV. Similarly, the C-p_z orbitals [Fig. 7(b)] become spin-polarized, where the spin-down channel is partially occupied, lying within an energy interval of around 0.5 eV above the Fermi level. Meanwhile, for negative EEF of -0.25 V/Å ($m = 0$), both spin-channels of Co-d_{z^2} and C-p_z become occupied, being resonant within 0.5 eV below the Fermi level.

In order to provide a more complete picture of the magnetic switching in Co[α^a]/GBL/Cu, we performed additional calculations of the electronic charge transfer and the net magnetic moment for another GBL–Cu(111) interface configuration, namely α_{hcp}-β_{top} [Fig. 1(c)]. We found practically the same values of CT and magnetic moment as those obtained for the energetically more stable α_{top}-β_{hcp} Co[α^a]/GBL/Cu system [Fig. 6], viz. CT of 8.6, 5.6, and 2.6×10^{13} e/cm^2, and $m = 0$, 0.40, and 0.74 μ_B for EEF of -0.25, 0, and +0.25 V/Å, respectively. Thus indicating that the proposed magnetic switching in Co[α^a]/GBL/Cu, tuned by an EEF, is not sensitive to the GBL–Cu(111) interface geometry. Indeed, in a recent experimental work, the author verified that the electronic properties of graphene "is not very sensitive" [16] to the relative atomic positions at the graphene/Cu interface.

IV. SUMMARY

In summary, we have performed an *ab initio* theoretical investigation of the substitutional cobalt defects in the bilayer graphene adsorbed on the Cu(111) surface. Initially, we verify the energetic stability of pristine graphene bilayer on Cu(111), GBL/Cu. The GBL becomes n-type doped, where the most of the charge transfer occurs on the (lower) graphene layer at the GBL–Cu(111) interface. By considering a free standing cobalt-doped GBL (Co/GBL), we find that there is an energetic preference for Co atoms in the α sites lying between the graphene layers (α^b). The net magnetic moment of Co/GBL is due to the unpaired Co-3d$_{z^2}$ and the C-p$_z$ orbitals neighboring the Co impurities. Upon its adsorption on Cu(111), Co/GBL/Cu, the charge transfer from the surface to the Co-doped GBL suppresses the magnetic moment of the Co/GBL. Furthermore, ruled by electrostatic interactions, different from the free-standing Co/GBL, in Co/GBL/Cu there is an energetic preference for substitutional cobalt impurities on the GBL surface, Co[α^a]/GBL/ and Co[β^a]/GBL/Cu. By applying an external electric field (EEF) the Co/GBL $\leftrightarrows$ Cu(111) charge transfer has been tuned in a suitable way, controlling the electronic occupation of the Co-d_{z^2} and C-p_z orbital near the Fermi level. The control of the electronic occupations allow us to switch on and off the net magnetic moment of Co[α^a]/GBL adsorbed on the Cu(111) surface. Further calculations suggest that such a magnetic switch properties in Co[α^a]/GBL/Cu do not depend of the GBL–Cu(111) interface geometry. Our study provides further support to the development of magnetic switch in 2D materials adsorbed on metallic surface, in particular, Co-doped GBL adsorbed on the Cu(111) surface.

ACKNOWLEDGMENT

The authors acknowledge financial support from the Brazilian agencies CAPES, CNPq, FAPEMIG, FAPES, and computational support from CENAPAD/SP.

[1] K. S. Novoselov, A. K. Geim, S. V. Morozov, D. Jiang, Y. Zhang, S. V. Dubonos, I. V. Grigorieva, and A. A. Firsov, Science **306**, 666 (2004).

[2] T. Ohta, A. Bostwick, T. Seyller, K. Horn, and E. Rotenberg, Science **313**, 951 (2006).

[3] A. K. Geim and I. V. Grigorieva, Nature (London) **499**, 419 (2013).

[4] H. Wang, Q. Wang, Y. Cheng, K. Li, Y. Yao, Q. Zhang, C. Dong, P. Wang, U. Schwingenschlögl, W. Yang, and X. X. Zhang, Nano Lett. **12**, 141 (2012).

[5] A. V. Krasheninnikov, P. O. Lehtinen, A. S. Foster, P. Pyykkö, and R. M. Nieminen, Phys. Rev. Lett. **102**, 126807 (2009).

[6] E. J. G. Santos, D. Sanchez-Portal, and A. Ayuela, Phys. Rev. B **81**, 125433 (2010).

[7] F. Donati, L. Gragnaniello, A. Cavallin, F. D. Natterer, Q. Dubout, M. Pivetta, F. Patthey, J. Dreiser, C. Piamonteze, S. Rusponi, and H. Brune, Phys. Rev. Lett. **113**, 177201 (2014).

[8] G. Giovannetti, P. A. Khomyakov, G. Brocks, V. M. Karpan, J. van den Brink, and P. J. Kelly, Phys. Rev. Lett. **101**, 026803 (2008).

[9] P. A. Khomyakov, G. Giovannetti, P. C. Rusu, G. Brocks, J. van den Brink, and P. J. Kelly, Phys. Rev. B **79**, 195425 (2009).

[10] I. Hamada and M. Otani, Phys. Rev. B **82**, 153412 (2010).

[11] M. Vanin, J. J. Mortensen, A. K. Kelkkanen, J. M. Garcia-Lastra, K. S. Thygesen, and K. W. Jacobsen, Phys. Rev. B **81**, 081408 (2010).

[12] T. Olsen and K. S. Thygesen, Phys. Rev. B **87**, 075111 (2013).

[13] J. Zheng, Y. Wang, L. Wang, R. Quhe, Z. Ni, W.-N. Mei, Z. Gao, D. Yu, J. Shi, and J. Lu, Sci. Rep. **3**, 2081 (2013).

[14] X. Li, W. Cai, J. An, S. Kim, J. Nah, D. Yang, R. Piner, A. Velamakanni, I. Jung, E. Tutuc, S. K. Banerjee, L. Colombo, and R. S. Ruoff, Science **324**, 1312 (2009).

[15] L. Gao, J. R. Guest, and N. P. Guisinger, Nano Lett. **10**, 3512 (2010).

[16] A. L. Walter, S. Nie, A. Bostwick, K. S. Kim, L. Moreschini, Y. J. Chang, D. Innocenti, K. Horn, K. F. McCarty, and E. Rotenberg, Phys. Rev. B **84**, 195443 (2011).

[17] J. D. Wood, S. W. Schmucker, A. S. Lyons, E. Pop, and J. W. Lyding, Nano Lett. **11**, 4547 (2011).

[18] K. Yan, H. Peng, Y. Zhou, H. Li, and Z. Liu, Nano Lett. **11**, 1106 (2011).

[19] L. Liu, H. Zhou, R. Cheng, W. J. Yu, Y. Liu, Y. Chen, J. Shaw, X. Zhong, Y. Huang, and X. Duan, ACS Nano **6**, 8241 (2012).

[20] S. Lee, K. Lee, and Z. Zhong, Nano Lett. **10**, 4702 (2010).

[21] P. Zhao, S. Kim, X. Chen, E. Einarsson, M. Wang, Y. Song, H. Wang, S. Chiashi, R. Xiang, and S. Maruyama, ACS Nano **8**, 11631 (2014).

[22] J. Zhang, J. Li, Z. Wang, X. Wang, W. Feng, W. Zheng, W. Cao, and P. Hu, Chem. Mater. **26**, 2460 (2014).

[23] Y. Xue, B. Wu, L. Jiang, Y. Guo, L. Huang, J. Chen, J. Tan, D. Geng, B. Luo, W. Hu, G. Yu, and Y. Liu, J. Am. Chem. Soc. **134**, 11060 (2012).

[24] M. Cattelan, S. Agnoli, M. Favaro, D. Garoli, F. Romanato, M. Meneghetti, A. Barinov, P. Dudin, and G. Granozzi, Chem. Mater. **25**, 1490 (2013).

[25] Y. Zhou, K. Yan, D. Wu, S. Zhao, L. Lin, L. Jin, L. Liao, H. Wang, Q. Fu, X. Bao, H. Peng, and Z. Liu, Small **10**, 2245 (2014).

[26] O. O. Brovko, P. Ruiz-Diaz, T. R. Dasa, and V. S. Stepanyuk, J. Phys.: Condens. Matter **26**, 093001 (2014).

[27] C. Gong, G. Lee, E. M. V. Bin Shan, R. M. Wallace, and K. Cho, J. Appl. Phys. **108**, 123711 (2010).

[28] R. R. Nair, I. L. Tsai, M. Sepioni, O. Lehtinen, J. Keinonen, A. V. Krasheninnikov, A. C. Neto, M. I. Katsnelson, A. K. Geim, and I. V. Grigorieva, Nat. Commun. **4**, 2010 (2013).

[29] M. M. Ugeda, D. Fernandez-Torre, I. Brihuega, P. Pou, A. J. Martinez-Galera, R. Pérez, and J. M. Gomez-Rodriguez, Phys. Rev. Lett. **107**, 116803 (2011).

[30] P. Hohenberg and W. Kohn, Phys. Rev. **136**, B864 (1964).

[31] W. Kohn and L. J. Sham, Phys. Rev. **140**, A1133 (1965).

[32] P. Giannozzi, S. Baroni, N. Bonini, M. Calandra, R. Car, C. Cavazzoni, D. Ceresoli, G. L. Chiarotti, M. Cococcioni, I. Dabo, A. D. Corso, S. de Gironcoli, S. Fabris, G. Fratesi, R. Gebauer, U. Gerstmann, C. Gougoussis, A. Kokalj, M. Lazzeri, L. Martin-Samos, N. Marzari, F. Mauri, R. Mazzarello, S. Paolini, A. Pasquarello, L. Paulatto, C. Sbraccia, S. Scandolo, G. Sclauzero, A. P. Seitsonen, A. Smogunov, P. Umari, and R. M. Wentzcovitch, J. Phys.: Condens. Matter **21**, 395502 (2009).

[33] J. P. Perdew, K. Burke, and M. Ernzerhof, Phys. Rev. Lett. **77**, 3865 (1996).

[34] We used the pseudopotentials Cu.pbe-d-rrkjus.UPF, C.pbe-rrkjus.UPF, and Co.pbe-nd-rrkjus.UPF, available from: www.quantum-espresso.org.

[35] A. M. Rappe, K. M. Rabe, E. Kaxiras, and J. D. Joannopoulos, Phys. Rev. B **41**, 1227 (1990).

[36] S. Grimme, J. Comp. Chem. **27**, 1787 (2006).

[37] H. J. Monkhorst and J. D. Pack, Phys. Rev. B **13**, 5188 (1976).

[38] R. Resta and K. Kunc, Phys. Rev. B **34**, 7146 (1986).

[39] K. Momma and F. Izumi, J. Appl. Cryst. **44**, 1272 (2011).

[40] In order to verify the reliability of our total energy results, we have calculated the adsorption energy (E^{ads}) of a graphene monolayer of the Cu(111) surface. We found $E^{\text{ads}} = 35.3\,\text{meV}/\text{Å}^2$ (100 meV/interface C atom); which compares very well with the experimentally obtained adsorption energy, of $45 \pm 4\,\text{meV}/\text{Å}^2$ (127 meV/interface C atom) [54].

[41] In order to verify the accuracy of our total energy results, we performed a set of additional calculations considering the recent rev-vdW-DF2 approach proposed by Hamada [55]. Within this approach, we found $E^{\text{ads}} = 25.5\,\text{meV}/\text{Å}^2$ (73 meV/interface C atom) for the α_{top}-β_{hcp} configuration; which is more stable by $0.3\,\text{meV}/\text{Å}^2$ (0.9 meV/interface C atom) than α_{hcp}-β_{fcc}, and $2.3\,\text{meV}/\text{Å}^2$ (6.5 meV/interface C atom) when compared with α_{hcp}-β_{top}. Thus confirming the energetic stability and energetic order presented in this work.

[42] S. D. Chakarova-Käck, A. Vojvodic, J. Kleis, P. Hyldgaard, and E. Schröder, New J. Phys. **12**, 013017 (2010).

[43] E. Mostaani, N. D. Drummond, and V. Fal'ko, Phys. Rev. Lett. **115**, 115501 (2015).

[44] Q. Wang, L. Wei, M. Sullivan, S.-W. Yang, and Y. Chen, RSC Adv. **3**, 3046 (2013).

[45] In order to verify the accuracy of the Cu(111)→ GBL charge transfers ($\Delta\rho$), we performed additional calculations by considering the following vdW approaches, rev-vdW-DF2 [55] and vdW-DF2-C09x [56]; where we found $\Delta\rho$ of 2.7 $(3.6)\times10^{13}e/\text{cm}^2$ and 4.0 $(5.3)\times10^{13}e/\text{cm}^2$, respectively, within the Bader (Löwdin) charge density analysis. Those results provide further support to the n-type doping of the BLG adsorbed on the Cu(111) surface. It is worth noting that $\Delta\rho$ is proportional to the BLG–Cu(111) equilibrium distance ($d_{\text{G-Cu}}$); namely by using the rev-vdW-DF2 and vdW-DF2-C09x we obtained $d_{\text{G-Cu}} = 3.30$ and 3.08 Å, respectively.

[46] C. Jeon, H.-N. Hwang, W.-G. Lee, Y. G. Jung, K. S. Kim, C.-Y. Park, and C.-C. Hwang, Nanoscale **5**, 8210 (2013).
[47] P. Dev and T. L. Reinecke, Phys. Rev. B **89**, 035404 (2014).
[48] Y. Tang, W. Chen, C. Li, W. Li, and X. Dai, J. Phys.: Condens. Matter **27**, 255009 (2015).
[49] R. F. W. Bader, *Atoms in Molecules: A Quantum Theory* (Oxford University Press, New York, 1990).
[50] W. Tang, E. Sanville, and G. Henkelman, J. Phys.: Condens. Matter **21**, 084204 (2009).
[51] M. Pashley, Phys. Rev. B **40**, 10481 (1989).
[52] J. E. Northrup and S. Froyen, Phys. Rev. B **50**, 2015 (1994).
[53] The effect of the EEF on the equilibrium geometry of GBL/Cu systems is quite negligible. By considering bias voltages between -0.25 and 0.50 V/Å, the atomic positions change by less than 0.001 Å.
[54] T. Yoon, W. C. Shin, T. Y. Kim, J. H. Mun, T.-S. Kim, and B. J. Cho, Nano Lett. **12**, 1448 (2012).
[55] I. Hamada, Phys. Rev. B **89**, 121103(R) (2014).
[56] V. R. Cooper, Phys. Rev. B **81**, 161104(R) (2010).